Science Advances
AAAS

Supplementary Materials for

Inhibition of ACLY overcomes cancer immunotherapy resistance via polyunsaturated fatty acids peroxidation and cGAS-STING activation

Wei Xiang *et al.*

Corresponding author: Hongyang Wang, hywangk@vip.sina.com; Wen Yang, woodeasy66@hotmail.com

Sci. Adv. **9**, eadi2465 (2023)
DOI: 10.1126/sciadv.adi2465

This PDF file includes:

Supplementary figures

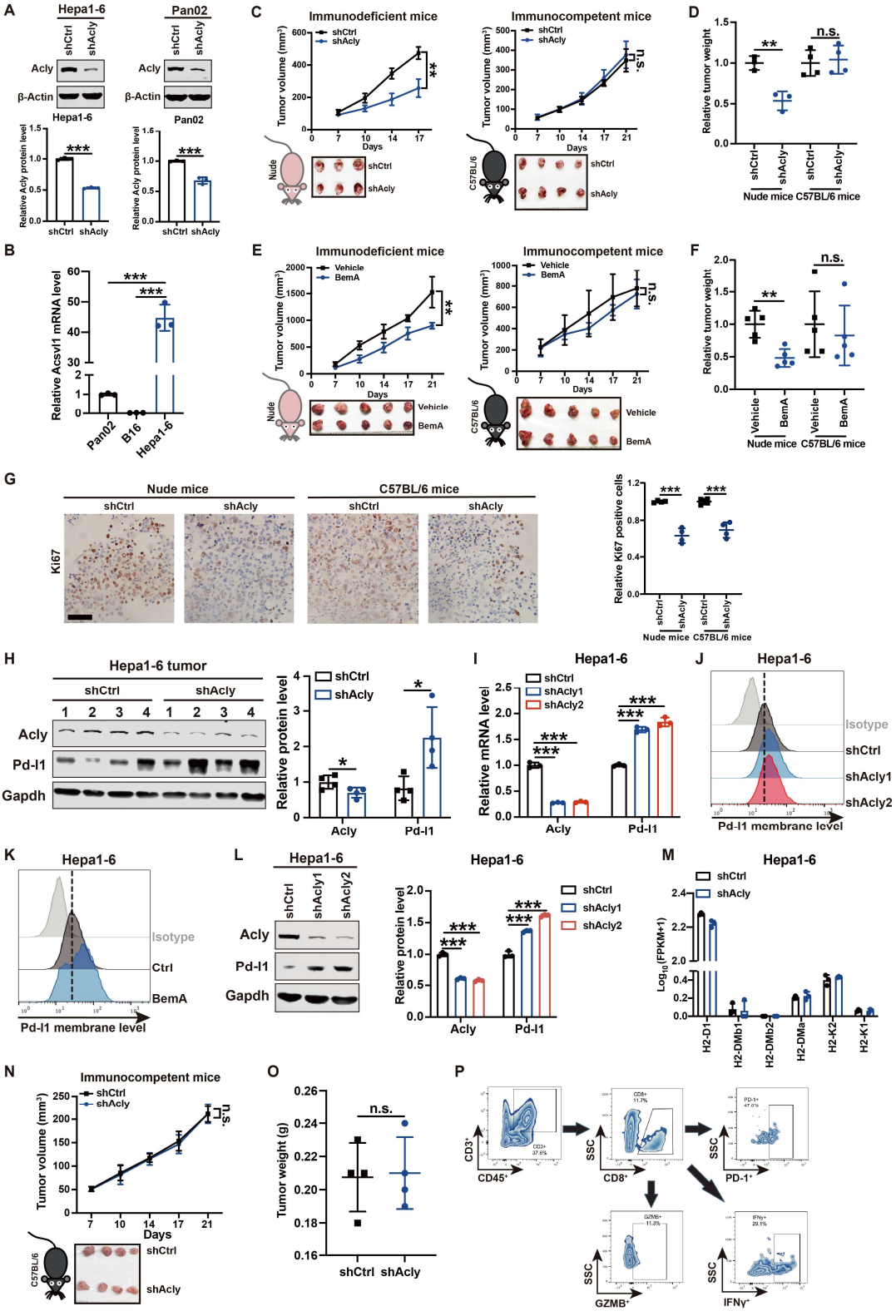

Fig. S1. ACLY inhibition compromises its anti-tumor effect in immunocompetent mice and upregulates PD-L1 expression in cancer cells. (**A**) Immunoblot analysis of Acly expression in Hepa1-6 cells and Pan02 cells with Acly knockdown or not. (**B**) qPCR analysis of Acsvl1 mRNA expressions in Pan02, B16, and Hepa1-6 cells. (**C** and **D**) Tumor growth (C) and relative tumor burdens (D) in immunodeficient nude mice and immunocompetent C57BL/6 mice injected subcutaneously with shAcly or shCtrl Hepa1-6 cells for 2-3 weeks. (**E** and **F**) Tumor growth (E) and relative tumor burdens (F) in immunodeficient nude mice and immunocompetent C57BL/6 mice injected subcutaneously with Hepa1-6 cells with treatment of ACLY inhibitor (BemA) or not for 2 weeks. (**G**) Immunohistochemical staining of Ki67 and quantification of Ki67 positive cells in shAcly or shCtrl Hepa1-6 tumors in immunodeficient nude mice and immunocompetent C57BL/6 mice. Scale bars, 100 μm. (**H**) Immunoblot analysis of Acly and Pd-l1 expression in Hepa1-6 tumors with Acly deficiency or not. (**I**) qPCR analysis of Acly and Pd-l1 mRNA expressions in Hepa1-6 cells with Acly knockdown or not. (**J** and **K**) Flow staining of surface Pd-l1 in Hepa1-6 cells with Acly knockdown (J) or BemA treatment (K). (**L**) Immunoblot analysis of Acly and Pd-l1 expressions in Hepa1-6 cells with Acly knockdown or not. (**M**) MHC-I mRNA expressions in Hepa1-6 shAcly cells versus shCtrl cells by RNA-seq. (**N** and **O**) Tumor growth (N) and tumor burdens (O) in C57BL/6 mice injected subcutaneously with shAcly or shCtrl Pan02 cells for 3 weeks. (**P**) The representative gating strategy used for flow cytometry analysis. n = 3 biological replicates from 3 independent experiments (A and L); n = 3 biological replicates from one independent experiment (B, I-K, and M); n = 3-5 mice per group from one independent experiment (C-F, N, and O); n = 4 biological replicates from one independent experiment (G and H). Statistical significance was assessed by unpaired *t* test (A, D, F-H, and O), one-way ANOVA (B, I, and L), and two-way ANOVA (C, E, and N); **P* < 0.05; ***P* < 0.01; ****P* < 0.001; n.s., not significant.

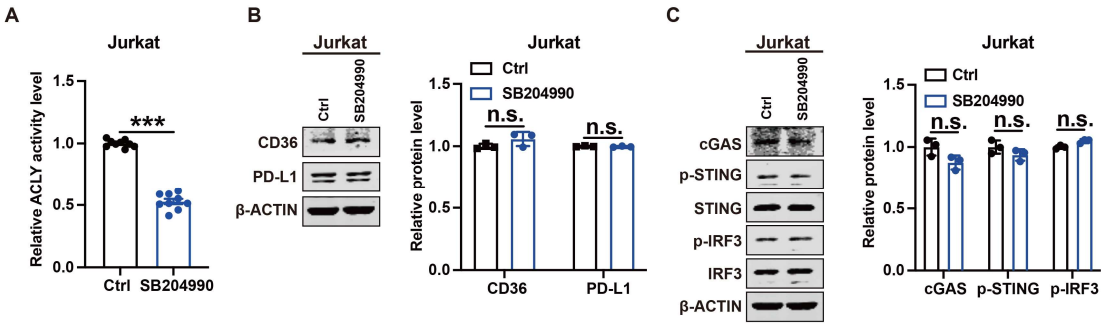

Fig. S2. ACLY inhibition has little impact on cGAS-STING activation in T cells. (**A**) Quantification of ACLY activity by ELISA in Jurkat cells with SB204990 treatment (20 μM) or not. (**B**) Immunoblot analysis of CD36 and PD-L1 expressions in Jurkat cells with SB204990 treatment (20 μM) or not. (**C**) Immunoblot analysis of cGAS, p-STING, STING, p-IRF3, and IRF3 expressions in Jurkat cells with SB204990 treatment (20 μM) or not. n = 9 biological replicates from 3 independent experiments (A) and data are shown as mean ± SEM; n = 3 biological replicates from 3 independent experiments (B and C). Statistical significance was assessed by unpaired *t* test (A-C); ****P* < 0.001; n.s., not significant.

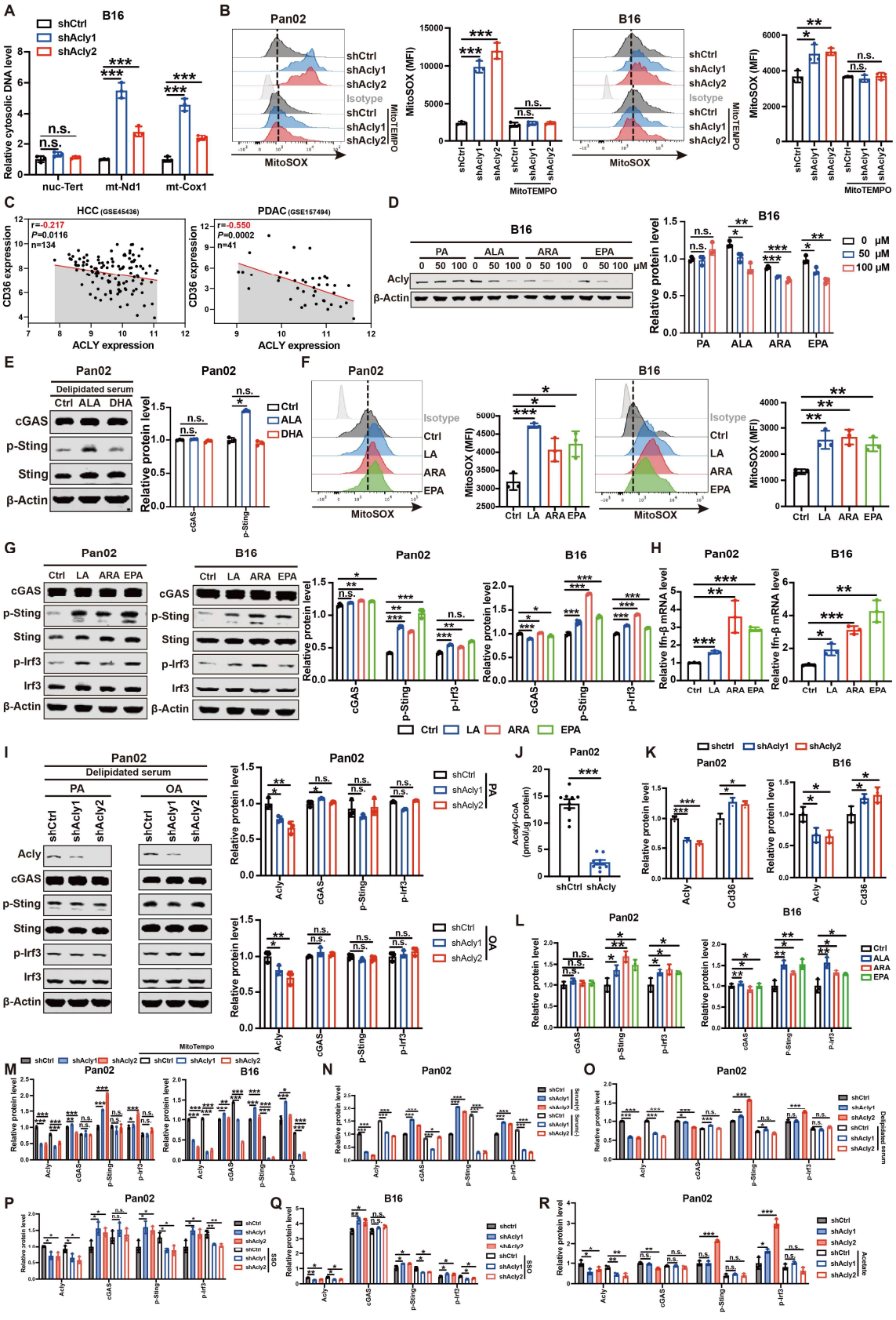
A
B16
shCtrl
shAcly1
shAcly2
Relative cytosolic DNA level
nuc-Tert
mt-Nd1
mt-Cox1
B
Pan02
MitoSOX
MitoSOX (MFI)
MitoTEMPO
Isotype
C
HCC (GSE45436)
r=-0.217
P=0.0116
n=134
PDAC (GSE157494)
r=-0.550
P=0.0002
n=41
CD36 expression
ACLY expression
D
PA
ALA
ARA
EPA
Acly
β-Actin
Relative protein level
0 μM
50 μM
100 μM
E
Delipidated serum
Ctrl ALA DHA
cGAS
p-Sting
Sting
F
Ctrl
LA
ARA
EPA
G
p-Irf3
Irf3
H
Relative Ifn-β mRNA level
I
PA
OA
J
Acetyl-CoA (pmol/μg protein)
K
Cd36
L
M
MitoTempo
N
O
Delipidated serum
P
Q
OSS
R
Acetate

Fig. S3. ACLY inhibition promotes PUFAs uptake to induce mitochondrial damage and cGAS-STING activation. (**A**) qPCR analysis of cytosolic DNA extracted from digitonin-permeabilized cytosolic extracts of B16 cells with Acly knockdown or not. (**B**) Flow staining and MFI of mitoSOX in Pan02 cells and B16 cells with Acly knockdown or not after mitoTEMPO treatment (10 μM). (**C**) Pearson's correlation between ACLY and CD36 expression in human HCC and PDAC datasets (n = 134 HCC patients, n = 41 PDAC patients). (**D**) Immunoblot analysis of Acly expression in B16 cells with PUFAs (ALA, ARA, or EPA) treatment (50 μM). (**E**) Immunoblot analysis of cGAS, p-Sting, Sting expressions in Pan02 cells with ALA or DHA treatment (50 μM). (**F**) Flow staining and MFI of mitoSOX in Pan02 cells and B16 cells with PUFAs (LA, ARA, or EPA) treatment (50 μM). (**G**) Immunoblot analysis of cGAS, p-Sting, Sting, p-Irf3, and Irf3 expressions in Pan02 cells and B16 cells with PUFAs (LA, ARA, or EPA) treatment (50 μM). (**H**) qPCR analysis of Ifn-β mRNA expression in Pan02 cells and B16 cells with PUFAs (LA, ARA, or EPA) treatment (50 μM). (**I**) Immunoblot analysis of Acly, cGAS, p-Sting, and p-Irf3 expressions in Pan02 cells with Acly knockdown or not after delipidated serum treatment with PA or OA supplementation (50 μM). (**J**) Quantification of acetyl-CoA contents by ELISA in Pan02 cells with Acly knockdown or not. (**K** to **R**) Qualification of protein bands in Fig. 4, B, H-L, and P. n = 3 biological replicates from one independent experiment (A, B, F, and H); n = 3 biological replicates from 3 independent experiments (D, E, G, I, and K-R); n = 9 biological replicates from 3 independent experiments (J) and data are shown as mean ± SEM. Statistical significance was assessed by one-way ANOVA (A, B, D-I, and K-R) and unpaired *t* test (J); **P* < 0.05; ***P* < 0.01; ****P* < 0.001; n.s., not significant.

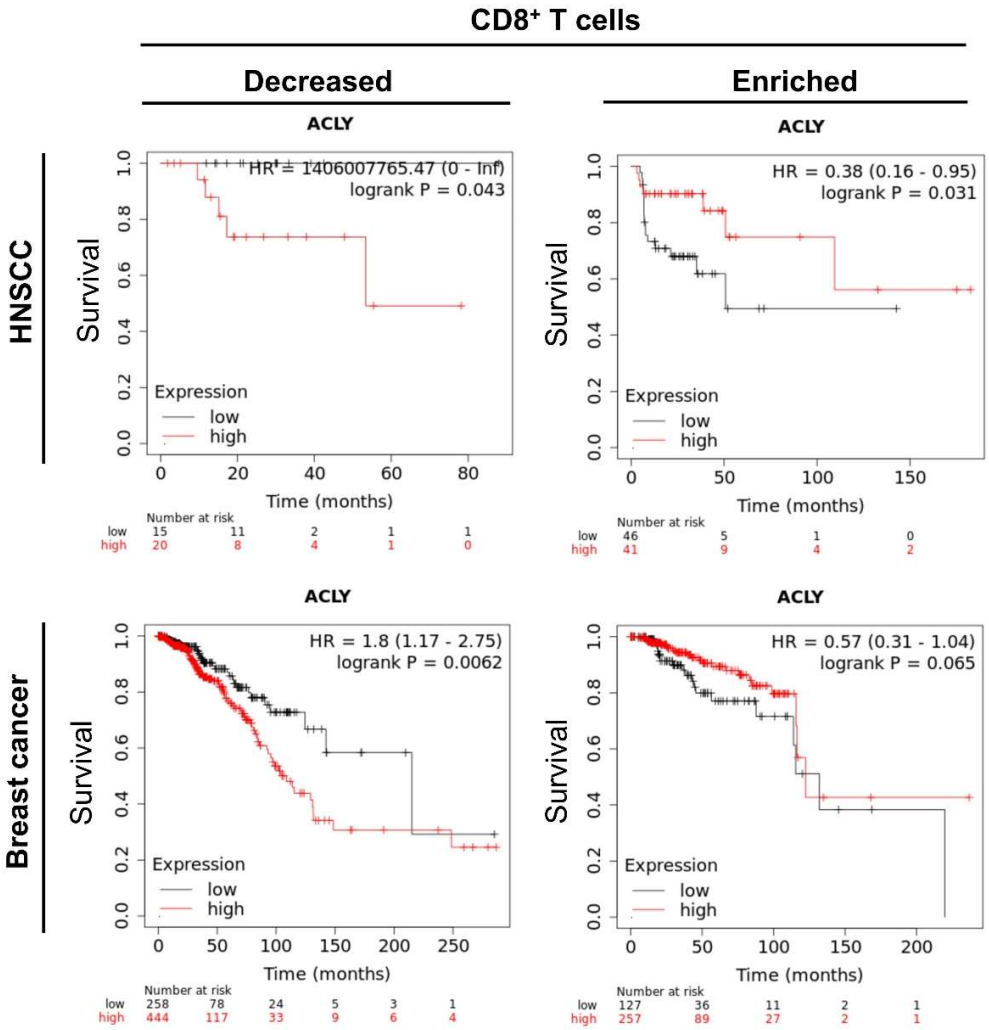

Fig. S4. Patients with low tumor ACLY expression in CD8⁺ T cell-enriched tumors have significantly poorer survival. (**A**) Kaplan-Meier analysis of survival in head and neck squamous cell carcinoma (HNSSC) and breast cancer patients according to the expression of ACLY in the group with decreased or enriched intratumoral CD8⁺ T cell infiltration.

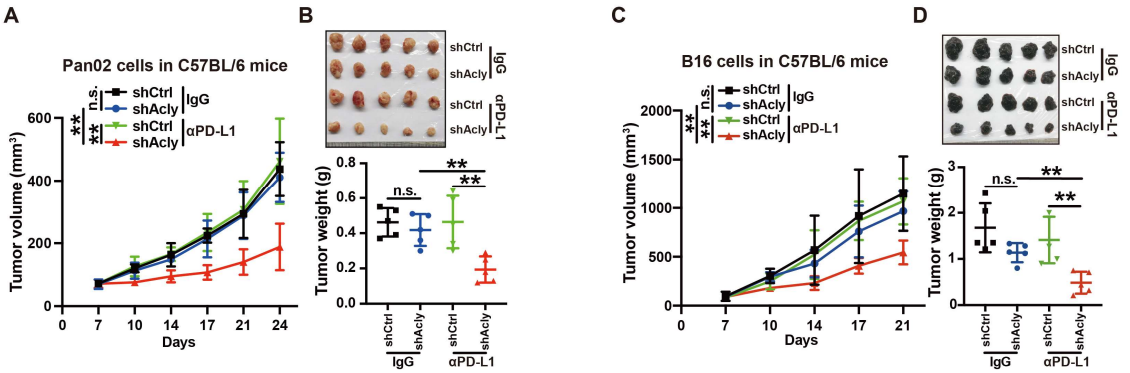

Fig. S5. ACLY inhibition overcomes cancer resistance to anti-PD-L1 therapy in melanoma. (**A** and **B**) Tumor growth (A) and tumor burdens (B) in C57BL/6 mice injected subcutaneously with shAcly or shCtrl Pan02 cells with αPD-L1 antibodies treatment. (**C** and **D**) Tumor growth (C) and tumor burdens (D) in C57BL/6 mice injected subcutaneously with shAcly or shCtrl B16 cells with treatment of αPD-L1 antibodies. n = 5 mice per group from one independent experiment (A-D). Statistical significance was assessed by two-way ANOVA (A and C) and one-way ANOVA (B and D); $^{**}P < 0.01$; n.s., not significant.

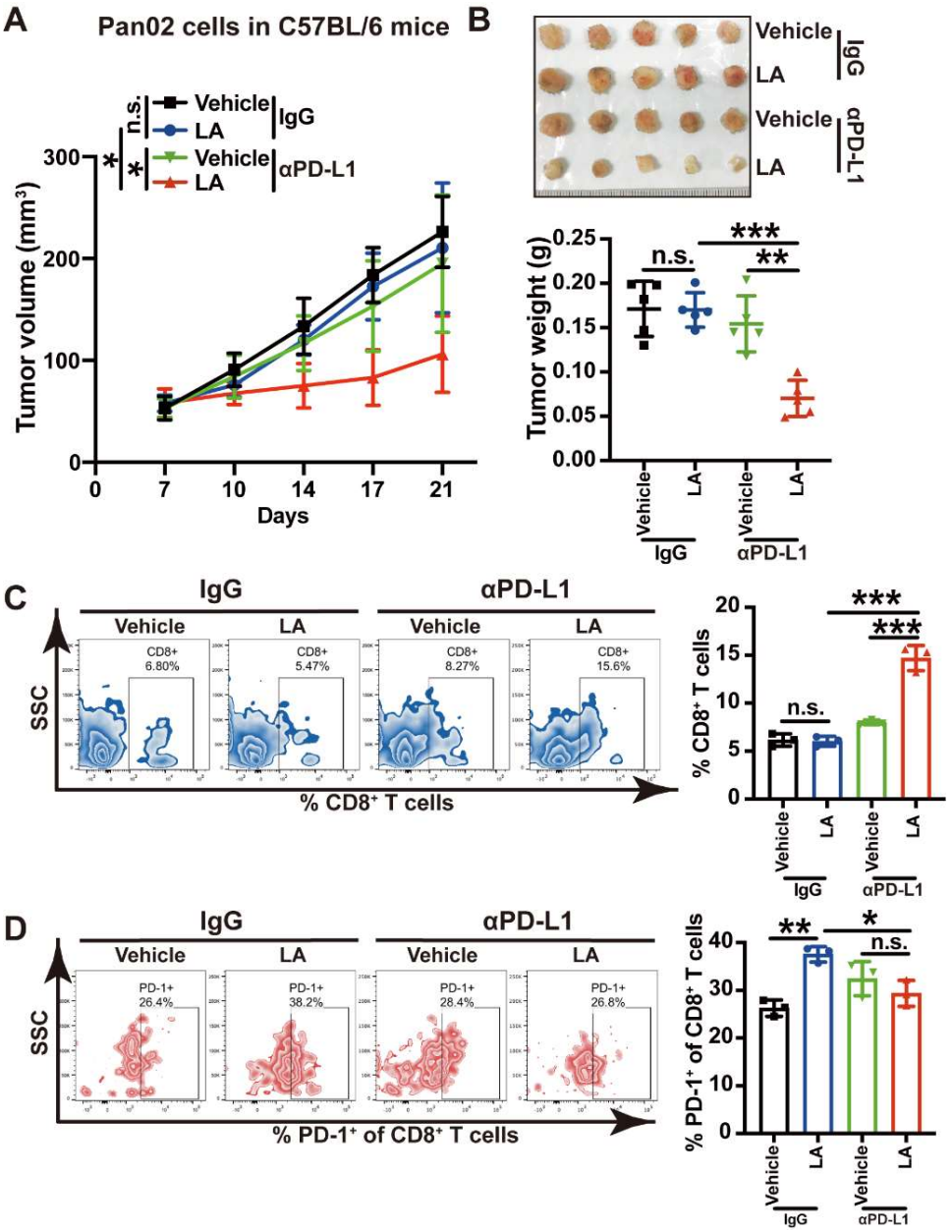

Fig. S6. Dietary LA supplementation enhances the efficacy of PD-L1 blockade. (**A** and **B**) Tumor growth (A) and tumor burdens (B) in C57BL/6 mice injected subcutaneously with Pan02 cells with treatment of LA and αPD-L1 antibodies either alone or in combination. (**C** and **D**) Flow staining and frequency of $CD8^+$ T cells (C) and $PD\text{-}1^+$ of $CD8^+$ T cells (D) in Pan02 tumors with treatment of LA and αPD-L1 antibodies either alone or in combination. n = 5 mice per group from one independent experiment (A and B); n = 3 biological replicates from one independent experiment (C and D). Statistical significance was assessed by two-way ANOVA (A) and one-way ANOVA (B-D); $^*P < 0.05$; $^{**}P < 0.01$; $^{***}P < 0.001$; n.s., not significant.